Environ. Sci. Technol. **2006**, *40,* 3813−3818

Influence of Sediment Components on the Immobilization of Zn during Microbial Fe−(Hydr)oxide Reduction

AARON J. COBY*,† AND FLYNN W. PICARDAL

Environmental Science Research Center, School of Public and Environmental Affairs, Indiana University, Bloomington, Indiana 47405

The fate of Zn and other sorbed heavy metals during microbial reduction of iron oxides is different when comparing synthetic Fe−(hydr)oxides and natural sediments undergoing a similar degree of iron reduction. Batch experiments with the iron-reducing organism *Shewanella putrefaciens* were conducted to examine the effects of an aqueous complexant (nitrilotriacetic acid or NTA), two solid-phase complexants (kaolinite and montmorillonite), an electron carrier (anthraquinone disulfonic acid or AQDS), and a humic acid on the speciation of Zn during microbial reduction of synthetic goethite. Compared to systems containing only goethite and Zn, microbial Fe(III) reduction in the presence of clay resulted in up to a 50% reduction in Zn immobilization (insoluble in a 2 h 0.5 M HCl extraction) without affecting Fe(II) production. NTA (3 mM) increased Fe(II) production 2-fold and resulted in recovery of nearly 75% of Zn in the aqueous fraction. AQDS (50 μM) resulted in a 12.5% decrease in Fe(II) production and a 44% reduction in Zn immobilization. Humic acid additions resulted in up to a 25% decrease in Fe(II) production and 51% decrease in Zn immobilization. The results suggest that all the components examined here as either complexing agents or electron shuttles reduce the degree of Zn immobilization by limiting the availability of Zn for incorporation into newly formed biogenic minerals. These results have implications for the remediation of heavy metals in a variety of natural sediments.

Introduction

The importance of dissimilatory reduction of iron oxide minerals has been documented for a large number of microorganisms in a range of environments (*1*−*3*). Microbial iron reduction is an important constituent of the global carbon and iron cycles (*4*−*8*) and has a profound effect on metal geochemistry in groundwater and sedimentary environments. A number of studies have examined the effect of natural and synthetic electron shuttles (*9*−*14*) and complexing agents (*15, 16*) on the extent and rate of microbial iron oxide reduction. In most cases the presence of an electron shuttle, such as humic acid or anthraquinone-2,6-disulfonic acid (AQDS), or complexing agent, such as nitrilotriacetic acid (NTA), results in an increase in the extent of iron reduction. In many cases, electron shuttles alleviate the need for direct contact between the bacterial and mineral surfaces (*9, 10*), and complexing agents may reduce the passivating effect of Fe(II) sorbed to those surfaces (*16*). Such effects suggest that the presence of these compounds may enhance not only iron reduction but also possibly any remediation activity stimulated by microbial iron reduction. Although the above studies have examined the effects of electron shuttles and complexants on rates, extent, or products of Fe(III) reduction, there have been few reports of their effects on the mobility of contaminant metals, such as Zn, during microbial iron reduction. The prevalence of analogous complexants and electron shuttles in subsurface environments and the potential for them to interact with contaminant metals suggests the need for such an examination.

Work by Cooper et al. has shown that the fate of the divalent metal, Zn, can be significantly affected by microbial reduction of goethite and lepidocrocite (*17, 18*). They reported that microbial iron reduction can lead to slightly elevated levels of aqueous Zn^{2+}, while concomitantly increasing the amount of adsorbed Zn that is insoluble in 0.5 M HCl (strongly bound or immobilized). The mechanism they proposed for this immobilization requires first that divalent Zn adsorb to the mineral surface before it is incorporated into new minerals formed during microbial iron reduction. Any substance, then, that affects the adsorption of Zn onto the iron mineral surface may affect the degree of immobilization. Cooper et al. have subsequently proposed that the presence of nonreducible adsorbing minerals in natural sediments, such as 1:1 clays, may be mitigating the immobilization of Zn by providing alternate sites for metal sorption, thus removing Zn from the iron oxide surface where immobilization occurs (*18*). While clays have been isolated as the probable cause for the inhibition of Zn immobilization in those sediments, the extent to which they are a mitigating factor has not been investigated. The ratio of clay surface to iron oxide surface varies between and within natural sediments. If clays act as a solid-phase complexant for Zn, then the greater the ratio of clay to iron oxide surface, the less Zn will be incorporated into biogenic minerals formed during microbial iron reduction. In addition, clays with different surface properties (e.g., expanding and nonexpanding) may exhibit different influences on the sorption and mobility of Zn.

Natural sediments are composed of a number of other compounds besides clays that influence metal geochemistry. Electron shuttling agents such as AQDS and humic acid have the ability to significantly alter Fe−(hydr)oxide reduction, and may significantly alter the degree of Zn bioimmobilization. In addition to functioning as electron shuttles, humic acids have multiple sites for cation complexation which could have an effect similar to that of clays on Zn immobilization. Thus, experiments utilizing pure, synthetic iron oxides, while often needed for understanding mechanisms, do not adequately address the complexity of natural sediments. It is the complexity of natural sediments, however, that makes interpretation of experimental results using them difficult. To address this problem, microbial iron reduction and heavy metal (Zn) speciation is examined here in pure, synthetic iron oxide systems that incorporate analogues of some individual components of natural sediments. This approach allows for a controlled examination of the geochemistry of systems more closely related to natural sediments while limiting the complexity. Specifically, the purpose of this study is to clarify how microbial Fe(III) reduction and the fate of Zn in Zn- and goethite-containing systems is influenced by solid- and aqueous-phase complexants (phyllosilicate clays,

* Corresponding author phone: (608) 890-0929; fax: (608) 262-0693; e-mail: coby@wisc.edu.

† Current address: Geology and Geophysics, Weeks Hall, University of Wisconsin, 1215 W. Dayton St., Madison, WI 53706.

10.1021/es0525197 CCC: $33.50
Published on Web 05/19/2006

NTA, and humic acid) and electron shuttles (AQDS and humic acid).

Experimental Methods

Microorganism and Culture Conditions. *Shewanella putrefaciens* is a Gram negative, motile rod with an obligate respiratory metabolism (*19*). The strain used in these experiments, *S. putrefaciens* 200, was originally isolated from a Canadian oil pipeline by Obuekwe (*20*). The culture was maintained on solid medium of nutrient agar containing 5 g L^{-1} yeast extract (Difco, Detroit, MI) as previously described (*21*). Liquid cultures were grown aerobically in a 1.0-L flask on a Lab Line shaker-table at 70 rpm in a medium that consisted (per liter) of 2.0 g of Na_2SO_4, 0.5 g of K_2HPO_4, 1.0 g of NH_4Cl, 0.198 g of $CaCl_2 \cdot 2H_2O$, 0.1 g of $MgSO_4 \cdot 7H_2O$, 19.35 mg of $FeCl_3 \cdot 6H_2O$, 0.5 g of yeast extract, and 3 mL of 60% (w/v) sodium lactate. *S. putrefaciens* cells were harvested by centrifugation and re-suspended in a cell concentrate to a target optical density ($A_{600} = \sim 1.2$) in artificial groundwater (AGW) medium. Small aliquots of this cell concentrate were subsequently used to inoculate the experimental slurries.

Iron Reduction Experiments with Zn and Goethite. The anoxic artificial groundwater (AGW) medium and synthetic high-surface-area (HSA) goethite used in these experiments has been described previously (*17, 18*). The AGW medium used in these experiments also contained 10 mmol L^{-1} HEPES buffer and 15 mmol L^{-1} lactate as a carbon source. An anoxic Zn stock solution was prepared by dissolving zinc chloride salt (Acros Organics) in Milli-Q water and adjusting to pH 6.0. Aliquots of the Zn stock were subsequently added to the AGW media so that the concentration of total exogenous Zn was either 175 or 250 μmol L^{-1}. Unless otherwise noted, the amount (0.09 g) of high-surface-area (HSA) goethite added to each acid-washed glass anaerobic culture tube (Bellco, 25 mL nominal volume) remained the same throughout all the experiments. This was equivalent to 50 mmol L^{-1} Fe(III) per tube as determined by citrate dithionate extraction. The tubes containing goethite were autoclaved and subsequently cooled in an anaerobic chamber (Coy Laboratory Products) containing 97% N_2 and 3% H_2. Under anaerobic conditions, 20 mL of lactate, HEPES, and Zn-amended, sterile AGW medium was added to the tubes. The tubes were then crimp-sealed with sterile, acid-washed butyl rubber stoppers and allowed to equilibrate, before inoculation, on a shaker table at 70 rpm (horizontal orientation) for a period of 18 h. The tubes were incubated on the shaker table throughout the experiment, and the sediment in the tubes was manually re-suspended once per day.

An initial set of samples (t_0) was taken for analysis immediately after inoculation with *S. putrefaciens*. Four sets of 5 tubes (3 inoculated and 2 uninoculated) were utilized for each sampling interval. For experiments examining the effect of clays, AQDS and NOM, samples were taken at day 0 immediately after inoculation and day 14. The experiment examining the effects of NTA had sampling events at days 0, 2, 7, and 14. For the purpose of comparison, all tubes are assumed to be equivalent aliquots of one large set. Fe(III) reduction experiments were initiated by inoculating slurries with 0.5 mL of *S. putrefaciens* suspension under anaerobic conditions. After dilution, this resulted in an estimated initial culture optical density (A_{600}) of 0.020, which corresponded to approximately 2×10^7 cells mL^{-1}. At each periodic sampling point, a set of tubes was removed and centrifuged (30 min, 4000*g*). The centrifuged tubes were then transferred to an anaerobic chamber, opened, and sampled for pH, aqueous Fe(II), and aqueous Zn. Aqueous Fe(II) was analyzed immediately via a modified version of the ferrozine technique (*22*) and aqueous Zn was acidified and stored for later analysis. Excess supernatant was decanted; the sediments were re-suspended in 20 mL of 0.5 M HCl and then transferred to a rotary mixer where they were digested for 2 h at room temperature. After digestion, the tubes were centrifuged again, and the supernatant was sampled for bound Fe(II) and Zn (bound = solid fraction that is soluble in 0.5 M HCl) (*17*). The procedure was repeated using 6.0 M HCl and digested for 24 h before sampling for strongly bound Zn (strongly bound = solid fraction that is not soluble in 0.5 M HCl). Acidified samples of supernatant for Zn analysis were stored in acid-washed polyethylene bottles for subsequent analysis via flame atomic absorption spectrophotometry (AAS). Total Zn was defined as the sum of aqueous, bound, and strongly bound species.

TABLE 1. Summary of Montmorillonite and Kaolinite Additions to Tubes Containing a Final Volume of 20 mL[a]

percent total surface area as clay	montmorillonite (g)	kaolinite (g)	clay surface area (m^2)
50	0.143		6
25	0.048		2
10	0.016		0.67
5	0.008		0.32
1	0.001		0.06
50		0.600	6
25		0.300	2
10		0.067	0.67
5		0.034	0.32
1		0.007	0.06
0			0

[a] Addition of each clay was made based on percent of the total mineral surface area (clay + goethite) in the system. The total surface area of goethite in each tube was approximately 6 m^2 (~0.09 g) based on a surface area of approximately 70 m^2/g (this study).

Experiments with NTA, AQDS, Clays, or Humic Acid. Stock solutions of NTA (0.5 M, pH 7) and AQDS (0.01 M) were prepared and sterilized by filtration through a 0.45 μm Osmonics cellulose filter. Aliquots of these stock solutions were then added to the AGW medium before inoculation with *S. putrefaciens*. The equilibrium speciation model, MINEQL+ (*23*), indicated that NTA preferentially complexed with Zn^{2+} over Fe^{2+} in our systems (data not shown). The final concentration of NTA in the tubes was 3 mM, which was estimated based on previous experiments to complex with all the Zn in the system and much of the Fe^{2+} produced over 14 days. The final concentration of AQDS used was 50 μM or approximately 20 mg/L.

For experiments examining the effect of clay on the degree of Zn immobilization, two different phyllosilicate clays, kaolinite (KGa-1b) and montmorillonite (SWy-1), were used. The two clays and information about their surface area were obtained from the Clay Minerals Society. Clay additions were based on the percent of total external-surface area in the system with goethite kept at a constant 50 mM (~6 m^2/tube). The internal (hydrated) surface area of the hydrated form of montmorillonite was not included in calculating the amount of clay to be added. The surface area of our high-surface-area (HSA) goethite was approximately 70 m^2/g as determined by multipoint Brunauer–Emmett–Teller (BET) N_2 adsoption on a NOVA 1000 surface area analyzer. The approximate surface area of the kaolinite and montmorillonite used in these experiments was 10 and 32 m^2/g, respectively. A summary of the clay amendments are presented for kaolinite and montmorillonite (Table 1). The clays were weighed and added to the tubes in the same manner as the goethite.

For experiments examining the effect that natural organic matter (NOM) had on the degree of Zn immobilization during the microbial reduction of iron minerals, a commercially available humic acid was used (Aldrich H1,675-2). A range

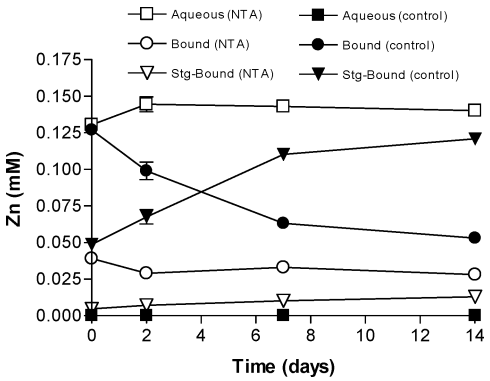

FIGURE 1. Zn speciation over 14 days incubation with *S. putrefaciens* in the presence (3 mM) (open symbols) and absence (filled symbols) of the chelator NTA. Total Zn added equaled 0.175 mM. Error bars indicate standard deviation of the means ($n = 3$). When not visible, error bars are obscured by data symbols. Stg-Bound represents strongly bound fraction.

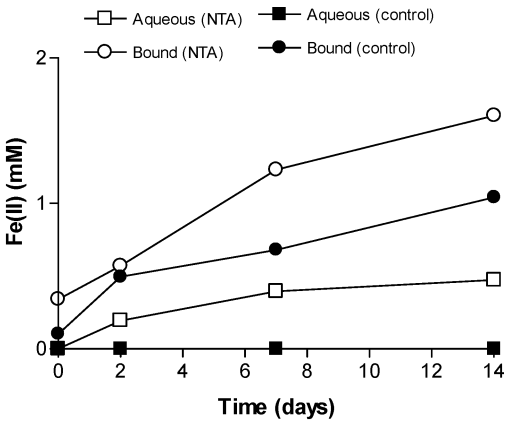

FIGURE 2. Bound and aqueous Fe(II) produced via the reduction of goethite after inoculation with *S. putrefaciens* in the presence (open symbols) and absence (filled symbols) of the chelator NTA. Error bars indicate standard deviation of the means ($n = 3$). Error bars are obscured by data symbols.

of concentrations was prepared to examine the effect of NOM: 50, 100, 250, and 400 mg/L. This range was chosen for comparative purposes to encompass the concentrations of NOM used in previous works (*9, 10, 14*).

Analyses. Solution pH was measured inside the anaerobic chamber. The concentration of Zn in acidified extracts was determined by flame AAS using a Perkin-Elmer 4100 flame atomic absorption spectrophotometer. Metal standards for AAS analysis were prepared by diluting aliquots of certified commercial standards in 0.5 M HCl. For colorimetric analysis of ferrozine-treated Fe(II) samples, the absorbance at 562 nm was measured on a Shimadzu UV-2101PC UV/VIS spectrophotometer. Unless otherwise noted, all solutions were prepared in Milli-Q water ($R = 18$ MΩ).

Results and Discussion

Effects of NTA Addition. Inoculated controls lacking NTA incorporated a significant amount of previously surface-sorbed Zn into a new biogenic mineral phase that was insoluble in a 2 h extraction of 0.5 N HCl (Figure 1). That immobilized Zn is referred to here as strongly bound Zn. Strongly bound Zn more than doubled after 14 days, while bound Zn (recovered in a 2 h, 0.5 N HCl extraction) decreased in proportion. A small amount of Zn (0.05 mM) is already strongly bound to the goethite at the initial time point. This is due to the 18 h equilibration of aqueous and solid phases before inoculation, during which time Zn may be diffusing into goethite micropores. Aqueous Zn concentrations remained very low and exhibited little change over time. In abiotic controls, aqueous, bound, and strongly bound Zn concentrations remained constant over the 14 day incubation period with nearly all the Zn (88%) recovered from the aqueous phase (data not shown). Results from experiments lacking NTA additions are in agreement with previous research by Cooper et al. examining the speciation of Zn during microbial goethite and lepidocrocite reduction (*17*).

In the systems containing 3 mM NTA, nearly all the Zn was recovered in the aqueous phase (~0.14 mM) throughout the experiment (open squares in Figure 1). At any time during the experiment, less than 19% of the total Zn was found in the bound phase and less than 8% of the total Zn was found in the strongly bound phase. NTA addition also resulted in a significant increase in the production of both aqueous and bound Fe(II) (Figure 2). The colorimetric method used for Fe(II) analysis is pH-sensitive; thus, the Fe(II) extracted with the 6 M HCl is not included in these results. After 14 days, approximately 2 times more Fe(II) was produced in systems with added NTA. This is in agreement with previous work by Urrutia et al. where the addition of 5 mM of NTA more than doubled the total (aqueous + adsorbed) Fe(II) produced after 15 days (*15*).

These results suggest a requirement that Zn be sorbed to the surface of the Fe−(hydr)oxide if it is to be subsequently immobilized in biogenic minerals. The formation of an aqueous Zn−NTA complex greatly reduced Zn sorption and prevented Zn immobilization. This supports the mechanistic hypothesis for Zn bioimmobilization proposed by Cooper et al. (*17*).

Effects of Clay Addition. After 14 days of incubation, the recovery of strongly bound Zn from uninoculated, montmorillonite-containing systems increased as the fraction of montmorillonite as total surface area increased (Figure 3a). The increase in strongly bound Zn was concurrent with a decrease in bound Zn. The change in aqueous Zn for both the montmorillonite and kaolinite systems was negligible and remained less than 0.004 mM in all cases. The increase in strongly bound Zn with increasing montmorillonite concentration may be due to the interlayer binding of Zn in montmorillonite. Zn bound in the interlayer may be resistant to the 2 h extraction with 0.5 M HCl, resulting in an apparent increase in strongly bound Zn. In contrast, strongly bound Zn in the uninoculated kaolinite systems remained stable with increasing addition of kaolinite (Figure 3b). Kaolinite does not expand when hydrated and would not support interlayer binding of Zn.

In inoculated montmorillonite systems, recovery of bound Zn increased with an increasing fraction of montmorillonite as total surface area and was accompanied by a decrease in recovery of strongly bound Zn (Figure 3a). In inoculated kaolinite systems, there was also a decrease in strongly bound Zn accompanied by an increase in bound Zn as clay additions increased (Figure 3b). A closer examination of the effect that montmorillonite and kaolinite additions had on the microbially mediated formation of strongly bound Zn is presented in Figures 4a and 4b. The values for strongly bound Zn in these figures are presented as the difference between strongly bound Zn from inoculated systems minus strongly bound Zn from uninoculated systems, and therefore represent the incorporation of Zn into a strongly bound state as a result of biological activity. Montmorillonite concentrations are inversely proportional to the degree of Zn bioimmobilization. When montmorillonite accounted for half of the total surface area in the system, there was approximately a 50% reduction in strongly bound Zn (~0.05 mM) relative to the clay-free control (Figure 4a). Strongly bound Zn in the kaolinite systems (Figure 4b) quickly declines by approximately 0.025 mM with increasing kaolinite concentration. The decrease in strongly

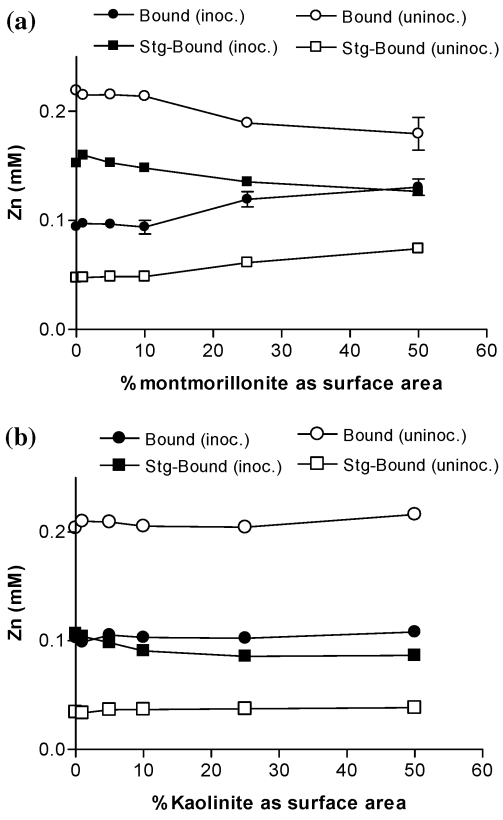

FIGURE 3. Zn speciation after 14 days incubation with *S. putrefaciens* (closed symbols) with increasing amendments of montmorillonite (a) or kaolinite (b). Uninoculated controls represented by open symbols. Aqueous concentrations of Zn for all treatments were under 0.004 mM and are omitted for clarity. Total Zn added equaled 0.25 mM. Error bars indicate standard deviation of the means ($n = 3$). Stg-Bound represents strongly bound Zn fraction.

bound Zn with kaolinite is half that of the decrease observed using montmorillonite. The results suggest that the effect of kaolinite is lessened after the kaolinite surface area equals 25% of the total surface area. Conversely, the presence of montmorillonite continued to have an effect on the formation of strongly bound Zn even after it accounted for 50% of the total external surface area (Figure 4a). There was little change in total Fe(II) production with increasing clay concentrations. Bound Fe(II) increased slightly as clay content increased, concurrent with a slight decrease in aqueous Fe(II) (Figure 5).

The presence of aluminum silicate clays had an effect similar to that of NTA on the bioimmobilization of Zn. As the ratio of clay to goethite increased, more Zn was likely bound to clay rather than goethite, even though >98% of Zn was sorbed in all cases. This resulted in a decrease in the Zn immobilized during microbial iron reduction. The clays in these systems appear to have functioned as a solid-phase complexant with Zn. The negatively charged surface of clays are known to complex with metal cations such as Zn^{2+} and Fe^{2+} (*15, 17, 24*−*26*). Urrutia et al. demonstrated in their study that aluminum oxides and layer silicates in direct contact with cells and goethite inhibited goethite reduction possibly due to the formation of aggregates, but when separated by a dialysis bag goethite reduction was enhanced (*15*). In the results presented here (Figure 5), the presence of montmorillonite did not facilitate or inhibit the reduction of goethite at any addition of clay. The dissimilarity in these results may be due to differences in the source of the clays and the total surface area in the systems. The inhibitory effect of clay on Zn immobilization, however, increased as the amount of clay surface area increased. Increasing the clay

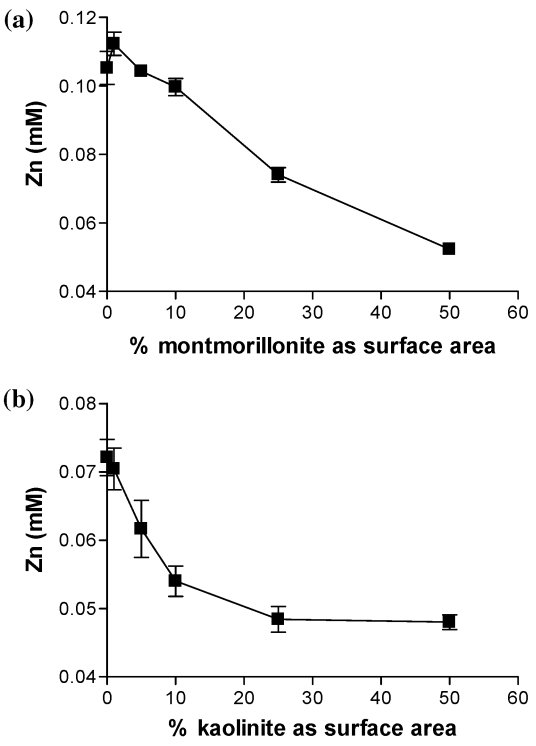

FIGURE 4. Strongly bound Zn after 14 days incubation with *S. putrefaciens* with increasing amendments of montmorillonite (a) or kaolinite (b). Values represent strongly bound Zn from inoculated system minus strongly bound Zn from uninoculated systems. Error bars indicate standard deviation of the means ($n = 3$).

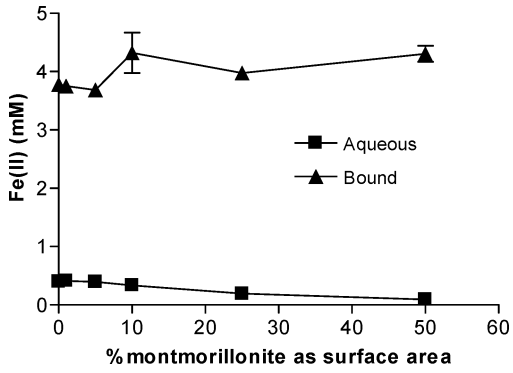

FIGURE 5. Fe(II) production with increasing amounts of montmorillonite after 14 days incubation with *S. putrefaciens*. Error bars indicate standard deviation of the means ($n = 3$). When not visible, error bars are obscured by data symbols.

content decreases the opportunity for Zn to be incorporated into new biogenic minerals generated during microbial reduction of goethite by offering additional sorptive surfaces that likely competitively reduce the amount of goethite-associated Zn. As suggested by Kukkadapu et al., it is also possible that Fe(II) sorption to clay surfaces reduces the degree of mineral formation by preventing Fe(II) saturation of the mineral surface (*27*), which would decrease the opportunity for Zn to be incorporated into new biogenic minerals.

To more easily compare surface areas between solid-phase additions, only the external surface of the montmorillonite was included in developing ratios for the total system surface area (clay and goethite) (Table 1). It was anticipated that the montmorillonite would exhibit a greater effect on the microbial immobilization of Zn than kaolinite because, when hydrated, the total surface area (internal + external) of montmorillonite potentially available for Zn sorption is

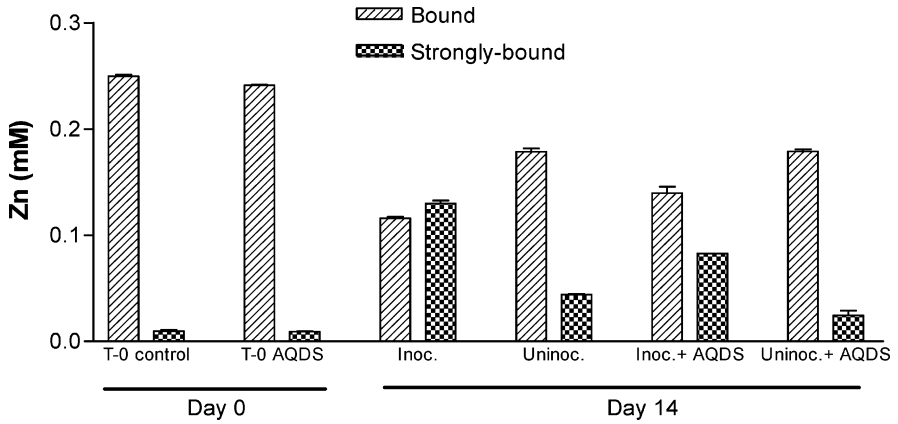

FIGURE 6. Zn speciation at time zero (T-0) and after 14 days incubation with *S. putrefaciens* in the presence and absence of the electron shuttle AQDS (50 μM). Aqueous values were all <0.008 mM and are omitted for clarity. Total Zn added equaled 0.25 mM. Inoc. = inoculated; Uninoc. = uninoculated.

between 40 and 100 times greater than that for kaolinite (*28, 29*). Indeed, the effect of montmorillonite on the formation of strongly bound Zn was twice that of kaolinite. This suggests that both the external and internal surface area of montmorillonite was involved as a surface complexant with Zn.

Effects of AQDS and Humic Acid Addition. After a 14 day incubation with and without 50 μM AQDS, approximately 4.0 mM (±0.14) Fe(II) was produced in the systems lacking AQDS whereas only 3.5 mM (±0.069) Fe(II) was produced in systems amended with AQDS (50 μM). The presence of AQDS also decreased the formation of strongly bound Zn. Approximately 44% less Zn was immobilized in the systems containing AQDS than in inoculated systems without AQDS relative to the uninoculated controls. These values correspond to a similar increase in bound Zn (Figure 6).

The addition of AQDS has been shown to increase the rate and extent of microbial Fe−(hydr)oxide reduction (*12, 14*). In the results presented here, AQDS addition to our Zn- and goethite-containing systems did not stimulate Fe−(hydr)-oxide reduction, but instead led to a partial inhibition of iron reduction. The exact mechanism for this inhibition is not known, but the decrease in iron reduction is at least partially responsible for the decrease in Zn immobilization. Stone found a similar inhibitory effect using hematite slurries, in which AQDS increased Fe(III) reduction in the absence of Zn, but when Zn was present, in even small quantities (<200 μM), no stimulation of Fe(III) reduction occurred (*30*). Stone noted that, in the presence of AQDS, Zn had a stronger affinity for adsorption to bacterial surfaces and suggested that the toxicity of Zn was increased, resulting in a decrease in Fe(III) reduction. An increase in Zn associated with bacterial surfaces would also decrease the Zn available for immobilization using the mechanism described by Cooper et al., which requires Zn to be sorbed to the iron mineral surface during microbial iron reduction (*17*).

The effect of humic acid amendments on the bioimmobilization of Zn is shown in Figure 7. As the concentration of humic acid was increased, the amount of strongly bound Zn decreased with a concurrent increase in bound Zn. Aqueous Zn was unaffected by humic acid amendments. When the humic acid concentration was 250 mg/L, the immobilization of Zn was decreased by 33%, and at 400 mg/L there was a 51% decrease in Zn immobilization compared to the inoculated controls with no humic acid amendment. In the uninoculated controls, addition of humic acid had no effect on the speciation of Zn. Increases in humic acid concentration decreased the total Fe(II) produced by 25% at the highest NOM concentration (Figure 8).

As with AQDS, additions of humic acid had a direct effect on the bioimmobilization of Zn relative to inoculated controls

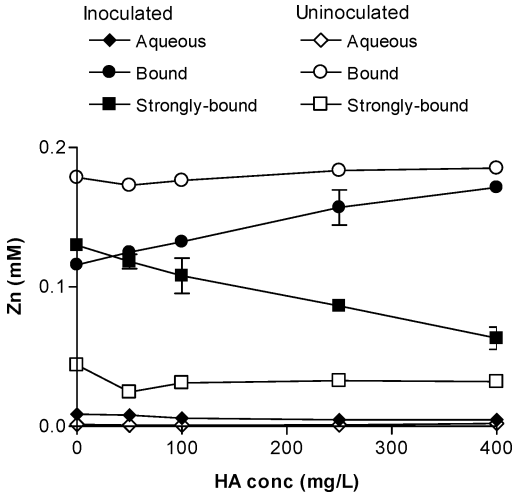

FIGURE 7. Zn speciation after 14 days incubation with (filled symbols) and without (open symbols) *S. putrefaciens* under increasing concentrations of humic acid. Error bars indicate standard deviation of the means (n = 3). Total Zn added equaled 0.25 mM. When not visible, error bars are obscured by data symbols.

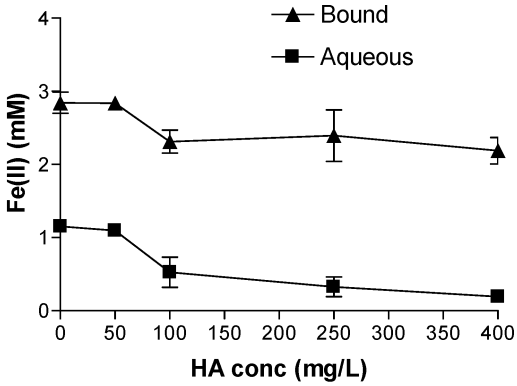

FIGURE 8. Fe(II) production after 14 days incubation with *S. putrefaciens* with increasing concentrations of humic acid. Error bars indicate standard deviation of the means (n = 3). When not visible, error bars are obscured by data symbols.

lacking humic acid (Figure 7). As the NOM concentration increased, so too did the inhibition of Zn immobilization. The increase in bound Zn and lack of change in aqueous Zn with increasing humic acid concentration suggests the formation and sorption of Zn−humic acid complexes. This hypothesis is supported by Spark et al. who reported that sorption of metals (including Zn) to the surface of goethite

is enhanced in the presence of humic acid, an observation explained by the sorption of Zn−humic complexes (*31*). In the results presented here, the putative Zn−humic acid complex bound to the goethite surface does not appear to allow for incorporation of Zn into any new biogenic minerals formed during microbial iron reduction. Removal of this humic-complexed Zn by 0.5 N HCl would explain the increase in bound Zn and decrease in strongly bound Zn, coinciding with the increase in humic acid concentration.

The addition of humic acid was anticipated to have a stimulatory affect on Fe−(hydr)oxide reduction as has been demonstrated by previous investigators (*10, 12, 14*). However, increases in humic acid concentration decreased the total Fe(II) produced by 25% at the highest NOM concentration (Figure 8). The sorption of Zn−humic and Fe(II)−humic complexes, and possibly the humic acid alone, onto the goethite surface may have reduced the number of surface sites available for Fe(III) reduction. This decrease in iron reduction may be responsible for some of the decrease in Zn immobilization, but does not account for the more than 50% reduction in Zn immobilization relative to the no-NOM control at the highest humic acid concentration. It therefore seems likely that the formation of surface-bound, Zn−humic acid complexes are also inhibiting the bioimmobilization of Zn by preventing Zn incorporation into new mineral assemblages.

As shown here, the presence of natural or anthropogenic complexants reduces the extent to which Zn is immobilized during microbial iron reduction. Aqueous- and solid-phase complexants such as NTA or phyllosilicate clays remove Zn from the goethite surface, thus preventing its incorporation into newly formed biogenic minerals. Large, complex compounds such as humic acid may also form complexes with Zn, which increases its affinity for sorption to bacterial and goethite surfaces. This may lead to both a decrease in the reduction of Fe(III) by surface passivation and the exclusion of Zn from Fe−(oxy)hydroxide surfaces where bacterial Zn immobilization occurs. These results underline the importance of understanding the influence of environmental conditions on the remediation of heavy metals in natural sediments.

Acknowledgments

We thank Dr. Craig Cooper for his helpful discussions and Dr. Deb Backhus for her contribution of clays and humic acid. We also thank the reviewers whose comments have greatly helped to improve this manuscript. This research was initially funded by a Department of Energy grant in Natural and Accelerated Bioremediation (DOE Grant No. DE-FG02-97ER62482), and continued support was provided by The School of Public and Environmental Affairs.

Literature Cited

(1) Lovley, D. R.; Anderson, R. T. Influence of dissimilatory metal reduction on fate of organic and metal contaminants in the subsurface. *Hydrogeol. J.* **2000**, *8*, 77−88.
(2) Lovley, D. R.; Holmes, D. E.; Nevin, K. P. Dissimilatory Fe(III) and Mn(IV) reduction. *Adv. Microb. Physiol.* **2004**, *49*, 219−287.
(3) Lloyd, J. R. Microbial reduction of metals and radionuclides. *Microbiol. Rev.* **2003**, *27*, 411−425.
(4) Fredrickson, J. K.; Gorby, Y. A. Environmental processess mediated by iron-reducing bacteria. *Curr. Opin. Biotechnol.* **1996**, *7*, 287−294.
(5) Konhauser, K. O. Diversity of bacterial iron mineralization. *Earth-Sci. Rev.* **1998**, *43*, 91−121.
(6) Lovley, D. R. Dissimilatory Fe(III) and Mn(IV) reduction. *Microbiol. Rev.* **1991**, *55*, 259−287.
(7) Lovley, D. R. Microbial Fe(III) reduction in subsurface environments. *FEMS Microb. Rev.* **1997**, *20*, 305−313.
(8) Lovley, D. R.; Phillips, E. J. Organic matter mineralization with reduction of ferric iron in anaerobic sediments. *Appl. Environ. Microbiol.* **1986**, *51*, 683−689.
(9) Chen, J.; Gu, B. H.; Royer, R. A.; Burgos, W. D. The roles of natural organic matter in chemical and microbial reduction of ferric iron. *Sci. Total Environ.* **2003**, *307*, 167−178.
(10) Lovley, D. R.; Fraga, J. L.; Blunt-Harris, E. L.; Hayes, L. A.; Coates, J. D. Humic substances as mediators for microbially catalyzed metal reduction. *Acta Hydrochim. Hydrobiol.* **1998**, *26*, 152−157.
(11) Nevin, K.; Lovley, D. Mechanisms for accessing insoluble Fe-(III) oxide during dissimilatory Fe(III) reduction of *Geothrix fermentans*. *Appl. Environ. Microbiol.* **2002**, *68*, 2294−2299.
(12) Nevin, K. P.; Lovley, D. R. Potential for nonenzymatic reduction of Fe(III) via electron shuttling in subsurface sediments. *Environ. Sci. Technol.* **2000**, *34*, 2472−2478.
(13) Newman, D. K.; Kolter, R. Role for excreted quinones in extracellular electron transfer. *Nature* **2000**, *405*, 94−97.
(14) Royer, R. A.; Burgos, W. D.; Fisher, A. S.; Jeon, B.; Unz, R. F.; Dempsey, B. A. Enhancement of hematite bioreduction by natural organic matter. *Environ. Sci. Technol.* **2002**, *36*, 2897−2904.
(15) Urrutia, M.; Roden, E.; Zachara, J. Influence of aqueous and solid-phase Fe(II) complexants on microbial reduction of crystalline iron(III) oxides. *Environ. Sci. Technol.* **1999**, *33*, 4022−4028.
(16) Urrutia, M.; Roden, E. Influence of biogenic Fe(II) on bacterial crystalline Fe(III) oxide reduction. *Geomicrobiol. J.* **2002**, *19*, 209−251.
(17) Cooper, D. C.; Picardal, F.; Rivera, J.; Talbot, C. Zinc immobilization and magnetite formation via ferric oxide reduction by *Shewanella putrefaciens* 200. *Environ. Sci. Technol.* **2000**, *34*, 100−106.
(18) Cooper, D. C.; Neal, A. L.; Kukkadupu, R. K.; Brewe, D.; Coby, A.; Picardal, F. W. Effects of sediment iron mineralogy on microbially mediated changes in divalent metal speciation: importance of ferrihydrite. *Geochim. Cosmochim. Acta* **2005**, *69*, 1739−1754.
(19) Semple, K. M.; Westlake, D. W. S. Characterization of iron-reducing *Alteromonas putrefaciens* strains from oil-field fluids. *Can. J. Microbiol.* **1987**, *33*, 366−371.
(20) Obuekwe, C. O. Microbial Corrosion of a Crude Oil Pipeline. Ph.D. Thesis, University of Alberta, Edmonton, Alberta, 1980.
(21) Picardal, F.; Arnold, R. G.; Couch, H.; Little, A. M.; Smith, M. E. Involvement of cytochromes in the anaerobic biotransformation of tetrachloromethane by *Shewanella putrefaciens* 200. *Appl. Environ. Microbiol.* **1993**, *59*, 3763−3770.
(22) Stookey, L. L. Ferrozine − a new spectrophotometric reagent for iron. *Anal. Chem.* **1970**, *42*, 779−781.
(23) Schecher, W.; McAvoy, D. *MINEQL+. A chemical equilibrium modeling program. Version 4.0*; Environmental research software: Hollowell, ME, 1998.
(24) Dimirkou, A.; Ioannou, A.; Papadopoulos, P.; Paschalidou, C. Zinc sorption by kaolinite: Influence of pH, electrolyte, and initial Zn concentrations with simultaneous release of Mg, Ca, Mn, and Cu ions. *Commun. Soil Sci. Plant Anal.* **2002**, *33*, 2917−2934.
(25) Ikhsan, J.; Johnson, B. B.; Wells, J. D. A comparative study of the adsorption of transition metals on kaolinite. *J Colloid Interface Sci.* **1999**, *217*, 403−410.
(26) Miranda-Trevino, J. C.; Coles, C. A. Kaolinite properties, structure and influence of metal retention on pH. *Appl. Clay Sci.* **2003**, *23*, 133−139.
(27) Kukkadapu, R. K.; Zachara, J. M.; Smith, S. C.; Fredrickson, J. K.; Liu, C. X. Dissimilatory bacterial reduction of Al-substituted goethite in subsurface sediments. *Geochim. Cosmochim. Acta* **2001**, *65*, 2913−2924.
(28) Helmy, A. K.; Ferreiro, E. A.; Bussetti, S. G. Surface area evaluation of montmorillonite. *J. Colloid Interface Sci.* **1999**, *210*, 167−171.
(29) Shen, Y.-H. Estimation of surface area of montmorillonite by ethylene oxide chain adsorption. *Chemosphere* **2002**, *48*, 1075−1079.
(30) Stone, J. J.; Burgos, W. D.; Royer, R. A.; Dempsey, B. A. Zinc and manganese inhibition of biological hematite reduction. *Environ. Engineer. Sci.*, in press.
(31) Spark, K. M.; Wells, J. D.; Johnson, B. B. Sorption of heavy metals by mineral-humic acid substrates. *Aust. J. Soil Res.* **1997**, *35*, 113−122.

Received for review December 16, 2005. Revised manuscript received April 21, 2006. Accepted April 21, 2006.

ES0525197